$1T$-TaS_2 charge-density-wave metal-insulator transition and Fermi-surface modification observed by photoemission

R. A. Pollak, D. E. Eastman, F. J. Himpsel, P. Heimann,* and B. Reihl
IBM Thomas J. Watson Research Center, Yorktown Heights, New York 10598
(Received 30 July 1981; revised manuscript received 25 September 1981)

A metal-to-insulator transition is observed using angle-resolved photoemission at the $1T_2 \rightarrow 1T_3$ phase transition of TaS_2 at $T \sim 200$ K: a 0.125-eV band gap, d subbands, and Fermi-surface modifications occur. High-resolution (0.15-eV) Ta $4f$ core-level spectra from $1T_3$-TaS_2 exhibit a charge-density-wave-induced splitting (0.73 eV) with only two narrow lines (0.25 eV full width) having an area ratio 0.70 ± 0.04, which is irreconcilable with current models that give three lines with a 6:6:1 intensity ratio.

The onset and phase transitions of charge density waves (CDW's) in transition-metal layered compounds continue to be of much interest.[1] Microscopic CDW theories, which presently do not exist, require a better understanding of the electronic structure of CDW phases.[2] Photoemission spectroscopy is a unique tool to probe this structure. Previous angle-resolved photoemission studies of $1T$-TaS_2 have reported the dispersion of the d^1 conduction band along the ΓM, ΓK, and MK[3,4] directions of the metallic room-temperature $1T_2$ phase and x-ray photoemission studies with 0.6-eV energy resolution have been used to determine the $1T_1$, $1T_2$, and $1T_3$ Ta $4f$ core-level splitting which is a measure of the CDW order parameter.[5,6]

Here we report angle-integrated and angle-resolved photoemission spectroscopy studies from the $1T_1$ incommensurate, $1T_2$ quasicommensurate, and $1T_3$ commensurate CDW phases of $1T$-TaS_2 which have been obtained at the Synchrotron Radiation Center of the University of Wisconsin using a two-dimensional (2D) display analyzer[7] (system resolution $\lesssim 0.15$ eV). Single crystals from the same batch used in Ref. 6, where the preparation procedure is described, were mounted with silver epoxy to a sample probe cooled with a Displex refrigerator which operated in the range 400 to 80 K.

Angle-integrated Ta $4f$ core-level spectra for $1T_1$, $1T_2$, and $1T_3$ phases of Ta_2 are shown in Figs. 1(a) and 1(b) for a photon energy $h\nu = 66$ eV. The Ta $4f_{7/2}$ peak is broad with an overall width of 1-eV full width at half-maximum (FWHM) in the $1T_1$ phase, it becomes split into two peaks of FWHM 0.5 eV in the $1T_2$ phase, and becomes split into two sharp peaks with equal FWHM of 0.25 eV in the $1T_3$ phase. The CDW is incommensurate with the lattice in $1T_1$ and $1T_2$, resulting in the observed broadening of the core levels. Binding energies are listed in Table I.

The pattern of peak splitting in commensurate $1T_3$ reflects the inequivalent potentials at Ta sites resulting from the triple-axis CDW configuration.[5,6] The $1T_3$ spectrum in Fig. 1(a) exhibits two Ta $4f_{7/2}$ components of equal FWHM $= 0.25 \pm 0.01$ eV separated by 0.73 ± 0.0005 eV with an area ratio[8] $A_{\alpha_2}/A_{\alpha_1} = 0.70 \pm 0.04$. Experimental signal-to-noise ratios were $\geq 200{:}1$. The absence of a third peak [see Fig. 1(b)] and the area ratio are irreconcilable with currently proposed 6:6:1, 1:6:6, and 6:7 (0.857) CDW configuration models.[5,6,9] Lower resolution XPS spectra have intensity ratios consistent with our results. If one assumes equivalent CDW configurations for all S-Ta-S sandwiches at the surface and into the bulk the same area ratio 0.70 ± 0.04 corresponds to a 5.3:7.7 ratio of α_2 and α_1 sites for a 13 atom layer unit cell. We have measured[8] the same $4f$ area ratio for the commensurate phase $1T$-$TaSe_2$ for which Brouwer and Jellinek[10] have used a 13 atom "Star-of-David" model to fit their x-ray diffraction results. This model leads to a 6:6:1 or 6:7 area ratios. They found $1T$-$TaSe_2$ to be triclinic with three equally probable twins responsible for the trigonal symmetry. The influence of the twins and the twin antiphase boundaries on the CDW configuration model might affect this ratio and explain the discrepancy with our results.

Helium beam atom diffraction[11] studies show a $\sqrt{13} \times \sqrt{13}$ superlattice for the topmost surface layer of $1T_3$-TaS_2 and are consistent with our assumption that the CDW configuration at the surface region is similar to that of the bulk. This assumption appears to be reasonable in view of the weak interlayer bonding and narrow observed $4f$ lines.

The 0.73-eV α_1-α_2 splitting of the two Ta $4f_{7/2}$ components can be used to estimate the amplitude of the CDW. A recent self-consistent renormalized atom model calculation[12] of the chemical shift of the core levels as a function of the number of valence d electrons in the solid finds a 15-eV/electron core-level shift. Thus our 0.73-eV splitting corresponds to a CDW amplitude of 0.05 electrons, which is much

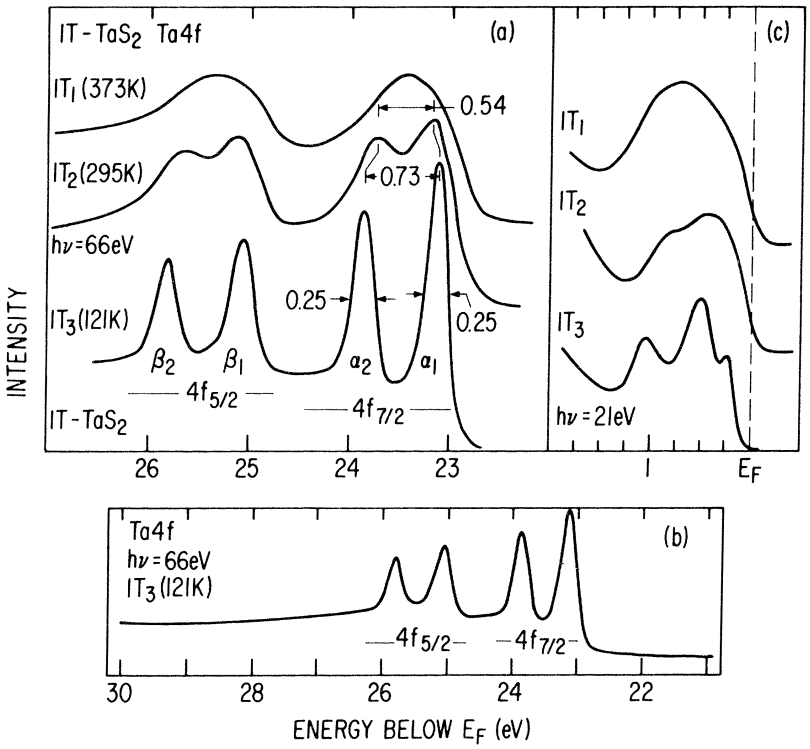

FIG. 1. (a) Ta $4f$ core-level spectra from different CDW phases of $1T$-TaS_2. (b) Ta $4f$ core-level wide scan from commensurate phase. (c) Angle integrated Ta "$5d^1$" conduction band.

smaller than a previous estimate of ~ 1 electron based on empirical chemical shift arguments.[5]

Angle-integrated "Ta $5d^1$" valence-band spectra are shown in Fig. 1(c). The overall bandwidth is ~ 1.1 eV for $1T_2$ and $1T_3$, with sharp subband structures and a gap at E_F appearing in the commensurate $1T_3$ spectrum. The top of the valence band, defined by the leading edge near E_F, moves down by a gap of 0.125 eV from E_F in the $1T_3$ phase. IR spectroscopy studies[13] did not find a sharp unique valence to conduction band gap, but suggested a broad "gap" of ~ 0.5 eV having a diminished state density.

The two-dimensional energy analyzer counts and displays all electrons emitted within a $\sim 80°$ cone of angles at a selected electron energy E and the component of electron momentum $\vec{k}$ parallel to the surface $\vec{k}_{\parallel}$ is conserved on crossing a smooth surface and is given by

$$|\vec{k}_{\parallel}| = (2\pi E/\hbar^2)^{1/2}\sin\theta \ ,$$

where θ is the polar angle between the photoelectron trajectory and the surface normal. Angle-resolved spectra ($h\nu = 21$ eV) along the ΓM direction for the $1T_2$ and $1T_3$ phases are shown in Fig. 2. In contrast with Ref. 3, emission is seen for all $\vec{k}_{\parallel}$ down to $\vec{k}_{\parallel}=0$ because mixed s/p polarization (rather than s polarization) was used, and normal emission ($\vec{k}_{\parallel}=0$) is only dipole allowed for p polarization because of the d_z^2 symmetry of the initial state. When the CDW

TABLE I. $1T$-TaS_2 Ta $4f$ binding energies relative to E_F(± 0.03 eV).

Phase	Ta $4f_{5/2}$			Ta $4f_{7/2}$	
	β_2	β_1	α_2		α_1
T_1	25.36			23.43	
T_2	25.65	25.11	23.72		23.18
T_3	25.78	25.05	23.85		23.12

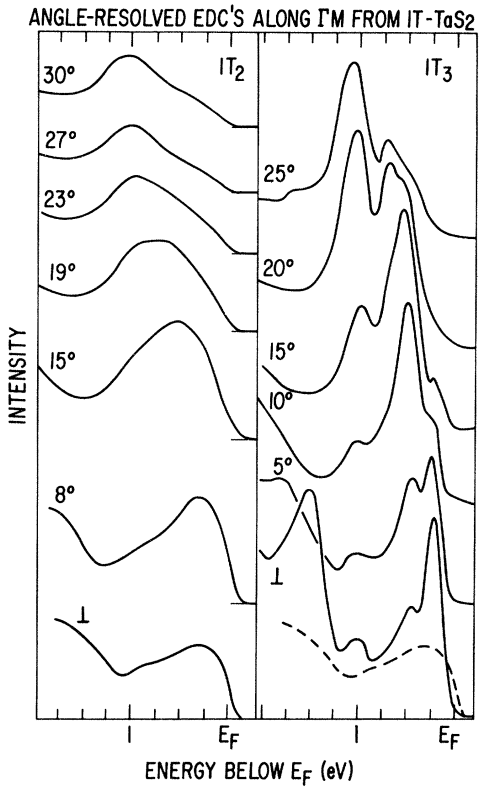

FIG. 2. Angle-resolved spectra from the quasicommensurate and commensurate phases of $1T$-TaS_2 in the ΓM direction. The $1T_2$ perpendicular emission curve is reproduced in the $1T_3$ panel (dashed line) for comparison.

becomes commensurate, sharp subband gapping occurs with the appearance of gap at E_F (compare dashed and solid curves for perpendicular emission) and with an increase in intensity in the uppermost peak. The $1T_2$ and $1T_3$ $\vec{k}_{\parallel}$-dependent valence-band spectra show a similarity in overall shape, i.e., if the $1T_3$ spectra are broadened by 0.3 eV, they would resemble the $1T_2$ spectra.

The peak nearest E_F in $1T_3$-TaS_2 [Fig. 1(c)] has a FWHM = 0.2 eV. The 0.125-eV insulating gap to E_F, this narrow peak, and the odd number 13 of Ta atoms in the layer unit cell suggests that the uppermost peak is from a localized state.[14] If this state was bandlike one would have a metallic behavior because the uppermost band would be half filled.

Because of the two-dimensional structure of

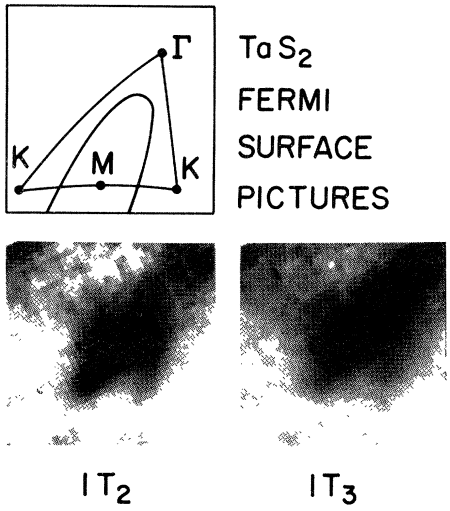

FIG. 3. Two-dimensional photoelectron images from the tail of states at E_F. Brillouin zone and Fermi surface distorted to correspond to 2D display analyzer response, image from quasicommensurate $1T_2$ phase, and image from commensurate $1T_3$ phase.

$1T$-TaS_2 parallel to the sample surface, two-dimensional photoelectron images taken with the 2D display analyzer set at E_F are projections of the elliptical cylinderlike Fermi surface from all planes to the ΓMK plane onto the detector plane. Figure 3 contains two such images, both from the tail of states at E_F. The flat regions of the Fermi surface where nesting can occur are projected onto the long part of the ellipses between M and K. Just this region is missing in Fig. 3 for both $1T_2$ and $1T_3$ phases.

In summary, the angle-resolved photomission data show that the charge-density wave reconstruction is associated with a metal-to-insulator transition which involves localized states in the insulating phase such as in an Anderson- or Mott-type localization. This transition could be triggered by a Fermi-surface instability since in the low-temperature phases we observe gaps of states in the regions where the high-temperature Fermi surface nests.

We thank Merrill Shafer for providing the TaS_2 and $TaSe_2$ crystals and the staff of the University of Wisconsin Synchrotron Radiation Center for their capable assistance.

*Present address: Ruhr Universität Bochum, Institüt für Experimentalphysik, AGR4 Oberflächenphysik, Universitätsstrasse 150, Gebäude NB, 4630-Bochum, West Germany.

[1]Review: R. H. Friend and D. Jerome, J. Phys. C 12, 1441 (1979).
[2]N. J. Doran, Physica (Utrecht) 99B, 227 (1980).
[3]M. M. Traum, N. V. Smith, and F. J. DiSalvo, Phys. Rev.

Lett. 32, 1241 (1974).
[4]R. Mamy, P. Thiry, G. Vachier, and A. Couget, J. Phys. (Paris) Lett. 42, L79 (1981).
[5]G. K. Wertheim, F. J. DiSalvo, and S. Chiang, Phys. Lett. 54A, 304 (1975).
[6]H. P. Hughes and R. A. Pollak, Philos. Mag. 34, 1025 (1976).
[7]D. E. Eastman, J. J. Donelon, N. C. Hien, and F. J. Himpsel, Nucl. Instrum. Methods 172, 327 (1980).
[8]The $1T$-TaS_2 Ta $4f$ area ratios were determined by a two-step spectral-decomposition procedure. First the Ta $4f_{5/2}$ peaks were stripped from the spectrum by subtracting a replica of the Ta $4f_{7/2}$ peaks shifted by a spin orbit splitting $\Delta_{SO}=1.925$ eV, scaled by a branching ratio $r_{SO}=0.65$ and lifetime broadened by convolution with a Lorentzian of FWHM $=0.05$ eV. The resulting Ta $4f_{7/2}$ CDW components were best separated using the same procedure with a separation of 0.73 eV, area ratio of 0.70 ± 0.04, and no lifetime broadening. We also obtained results for $1T$-$TaSe_2$ which had the same Δ_{SO}, r_{SO}, and CDW area ratio with a smaller peak separation of 0.66 eV.
[9]J. A. Wilson, Phys. Rev. B 17, 3880 (1978).
[10]R. Brouwer and F. Jellinek, Physica (Utrecht) 99B, 51 (1980).
[11]P. Cantini, G. Boato, and R. Colella, Physica (Utrecht) 99B, 59 (1980).
[12]M. C. Desjonqueres, D. Spanjaard, Y. Lassailly, and C. Guillot, Solid State Commun. 34, 807 (1980).
[13]A. S. Barker, Jr., J. A. Ditzenerger, and F. J. DiSalvo, Phys. Rev. B 12, 2049 (1975).
[14]P. Fazekas and E. Tosatti, Philos. Mag. B 39, 229 (1979).

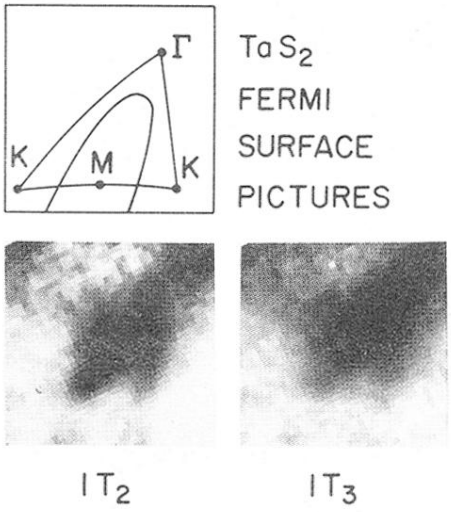

FIG. 3. Two-dimensional photoelectron images from the tail of states at E_F. Brillouin zone and Fermi surface distorted to correspond to 2D display analyzer response, image from quasicommensurate $1T_2$ phase, and image from commensurate $1T_3$ phase.